JOURNAL OF THE ROYAL SOCIETY INTERFACE

Experimental degradation of helicoidal photonic nanostructures in scarab beetles (Coleoptera: Scarabaeidae): implications for the identification of circularly polarizing cuticle in the fossil record

Journal:	*Journal of the Royal Society Interface*
Manuscript ID	rsif-2018-0560.R2
Article Type:	Research
Date Submitted by the Author:	n/a
Complete List of Authors:	Odin, Giliane; University College Cork School of Biological Earth and Environmental Sciences, McNamara, Maria; University College Cork, School of Biological, Earth and Environmental Sciences Arwin, Hans; Linkopings universitet, Department of Physics, Chemistry and Biology Järrendahl, Kenneth; Linkopings universitet, Department of Physics, Chemistry and Biology
Categories:	Life Sciences - Earth Science interface
Subject:	Evolution < CROSS-DISCIPLINARY SCIENCES, Biomaterials < CROSS-DISCIPLINARY SCIENCES
Keywords:	structural colours, Bouligand structure, taphonomy, fossil insects, Mueller-matrix ellipsometry

Under review for J. R. Soc. Interface

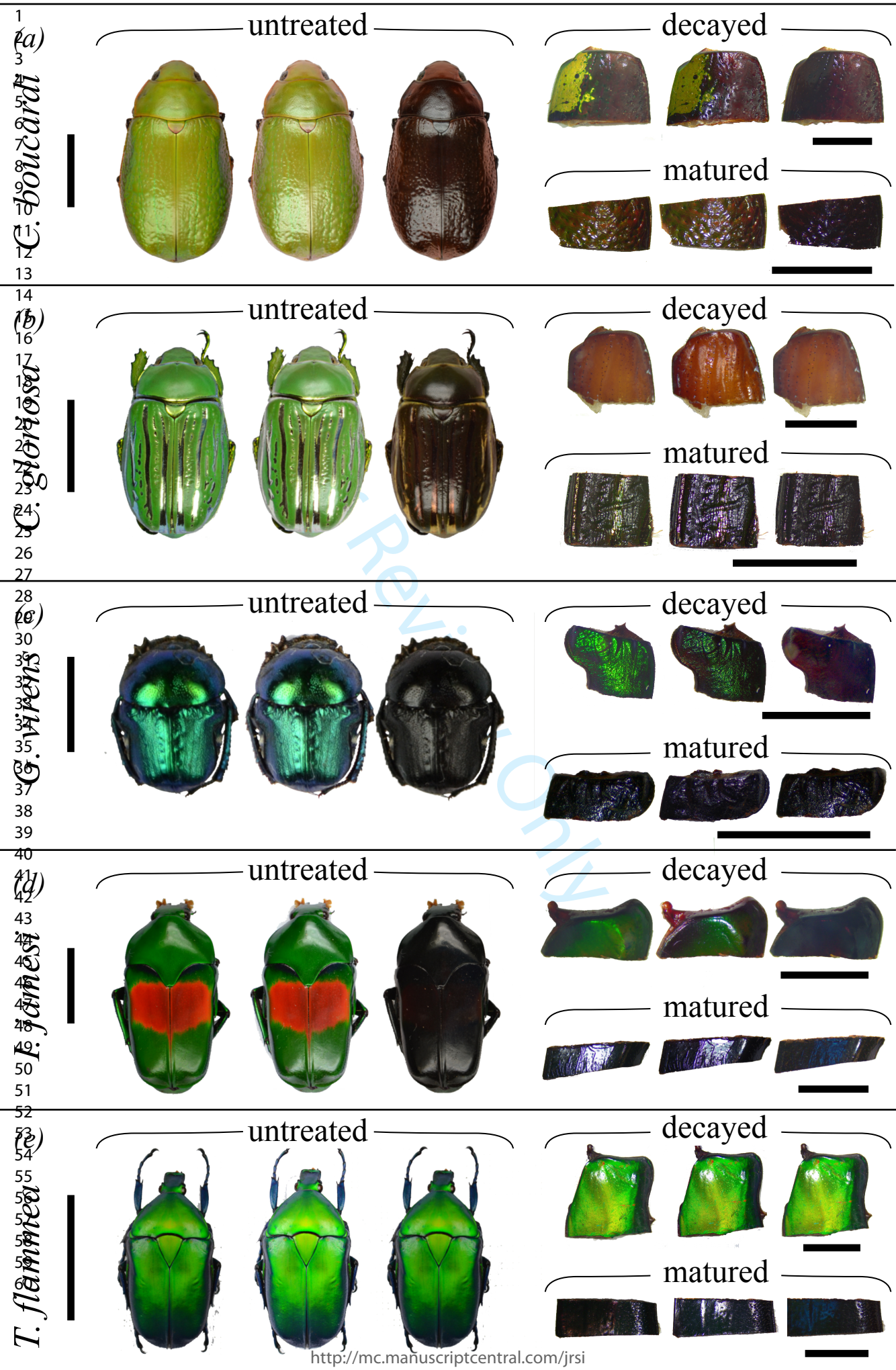

For Review Only

Figure 1

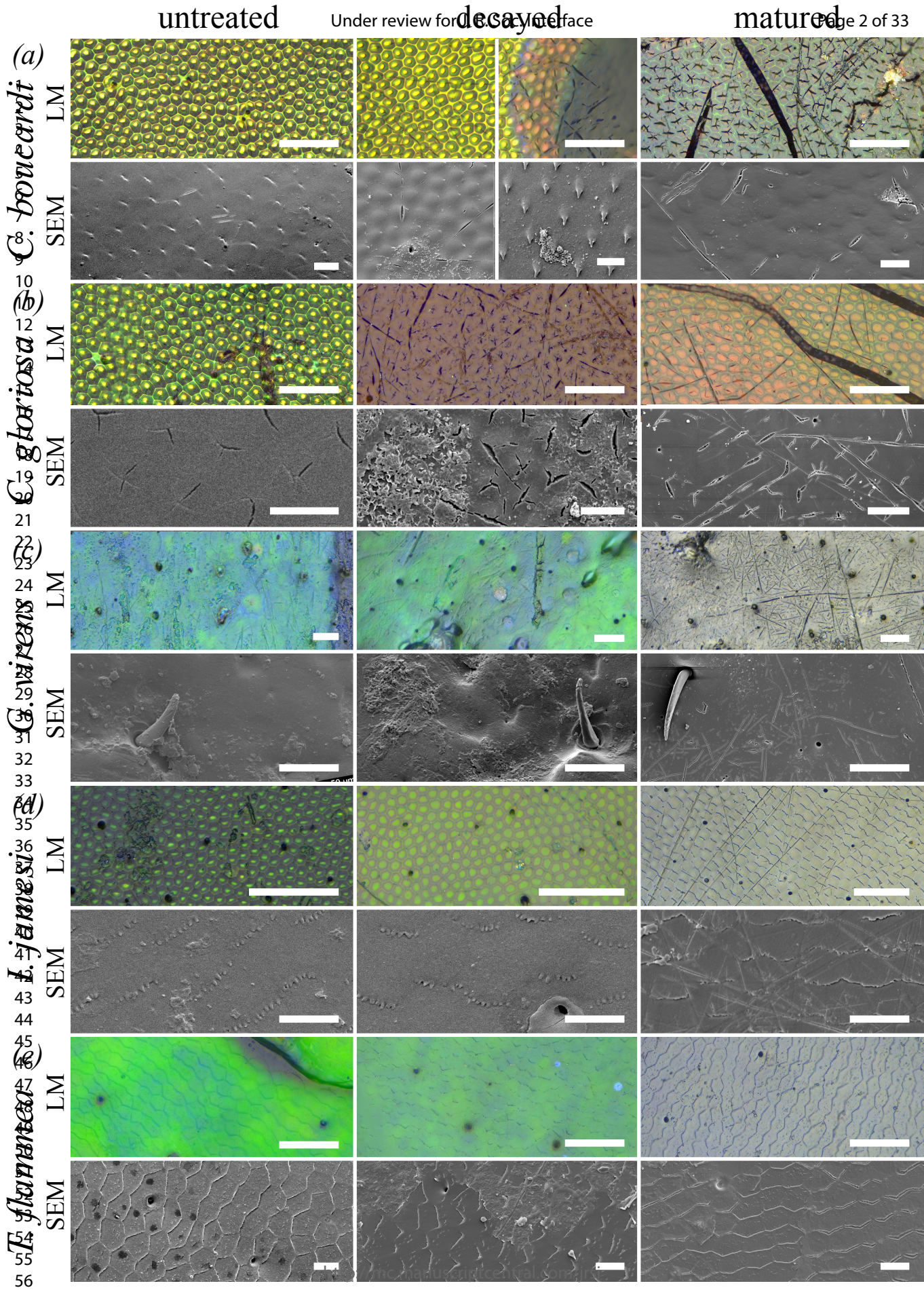
untreated
decayed
matured
(a)
C. boucardi
LM
SEM
(b)
C. glauca
LM
SEM
(c)
C. winsemanii
LM
SEM
(d)
L. jamesii
LM
SEM
(e)
T. flammeum
LM
SEM

Figure 2

Figure 3

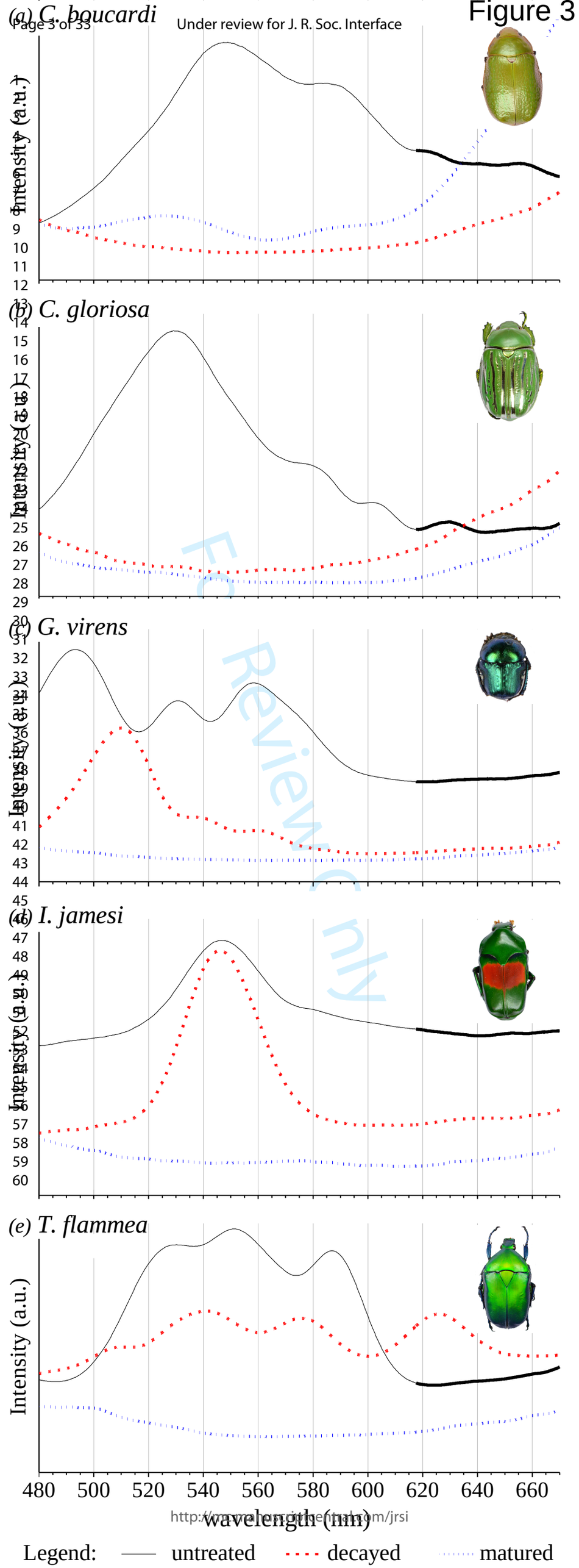

For Review Only

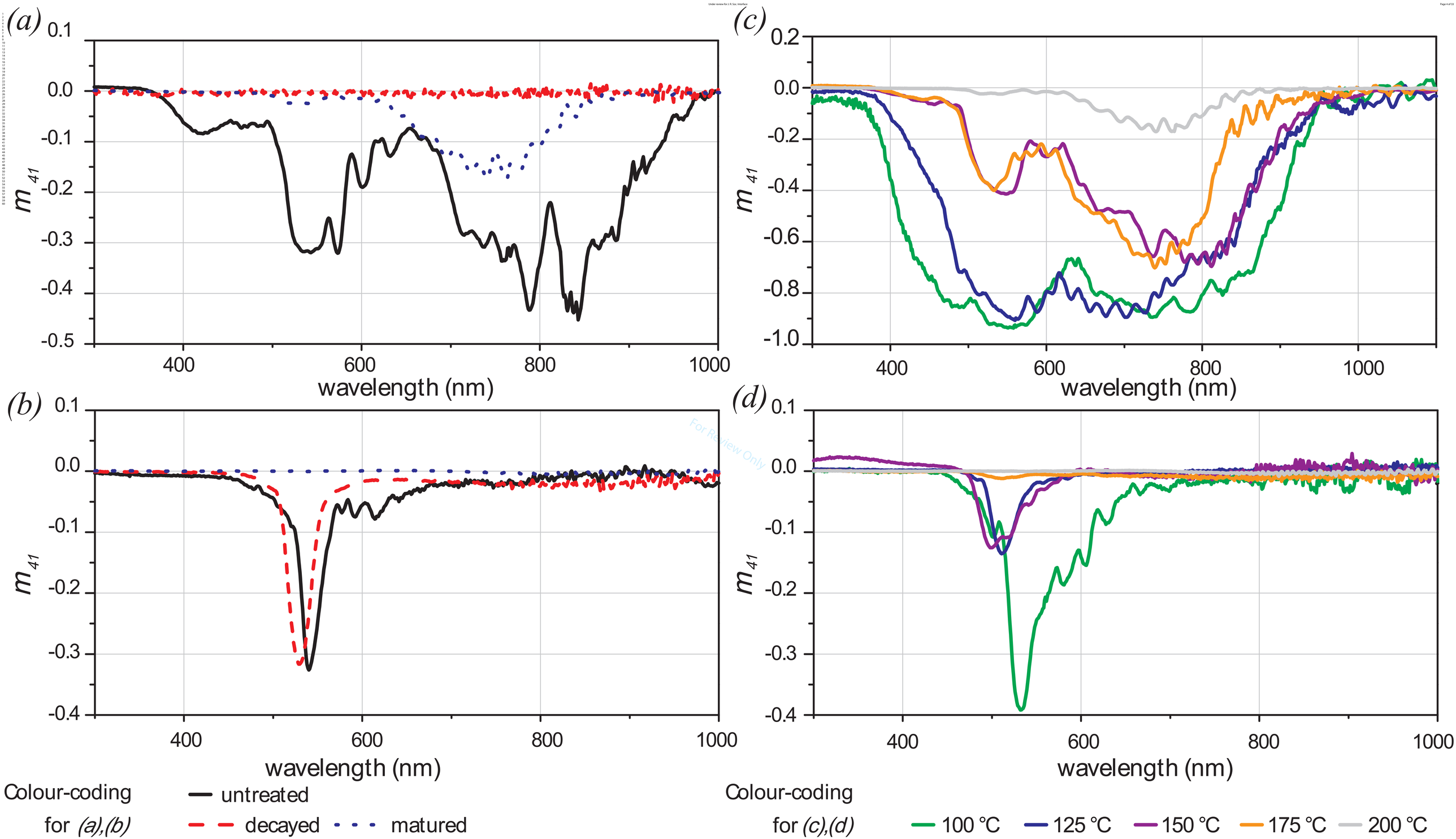

Figure 4

For Review Only

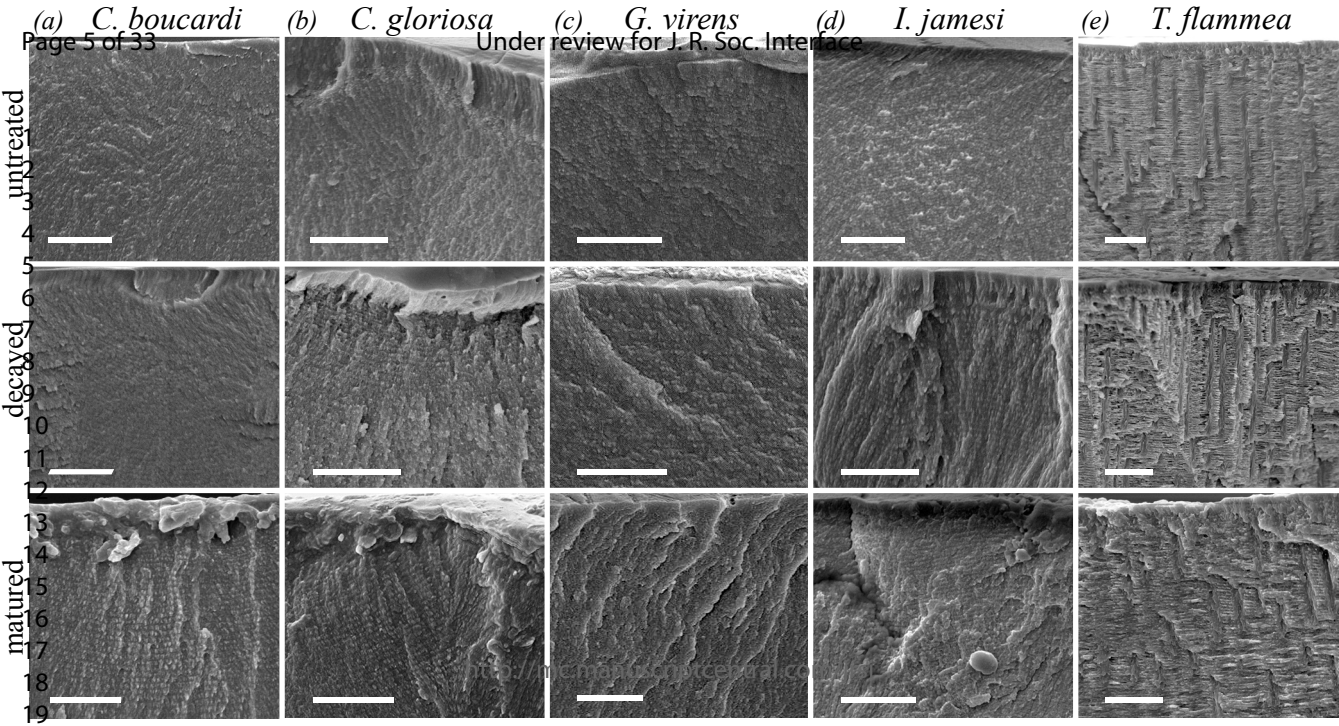
(a) C. boucardi
(b) C. gloriosa
(c) G. virens
(d) I. jamesi
(e) T. flammea
untreated
decayed
matured

Figure 5

http://mc.manuscriptcentral.com/jrsi

S1 Figure 1

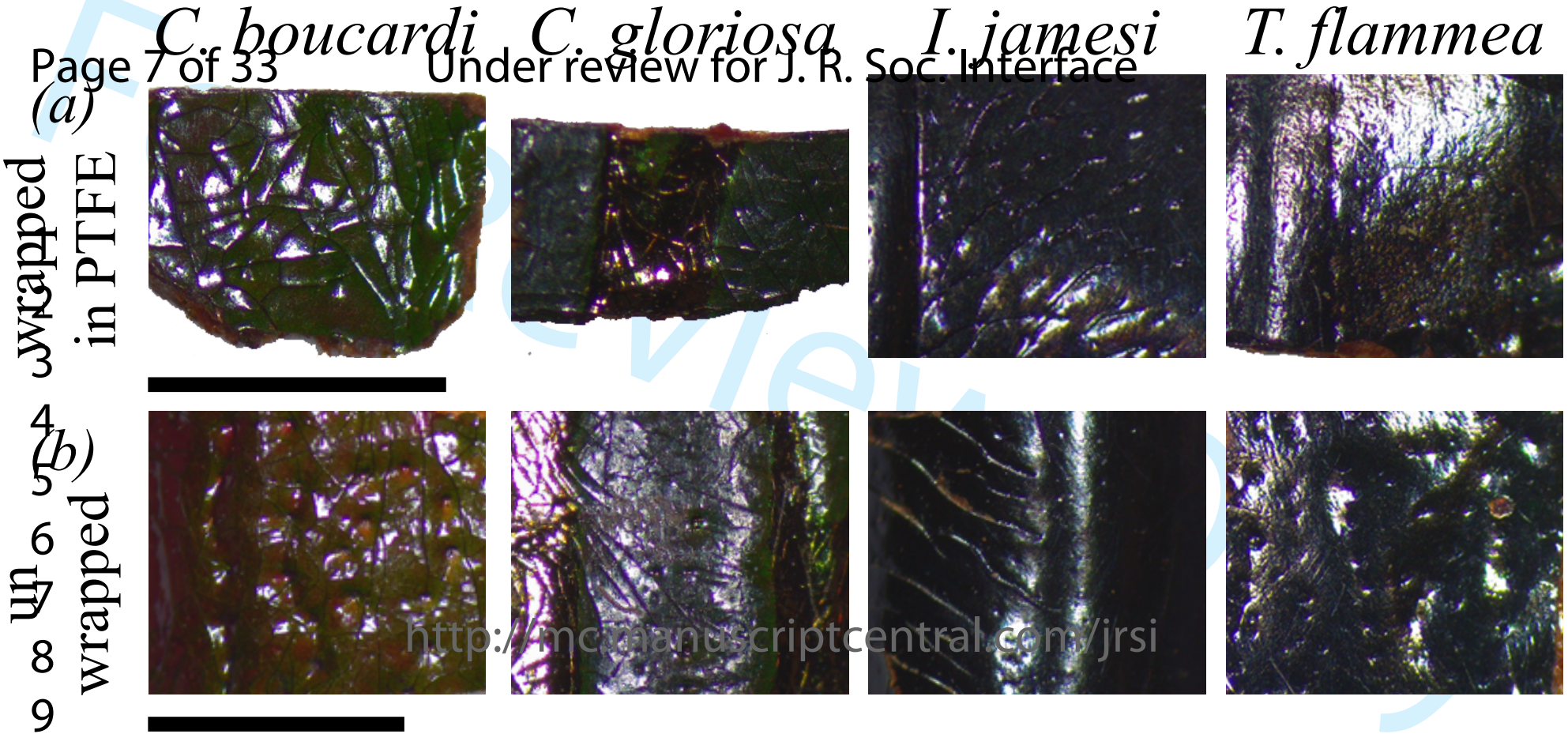

http://mc.manuscriptcentral.com/jrsi

Figure 2

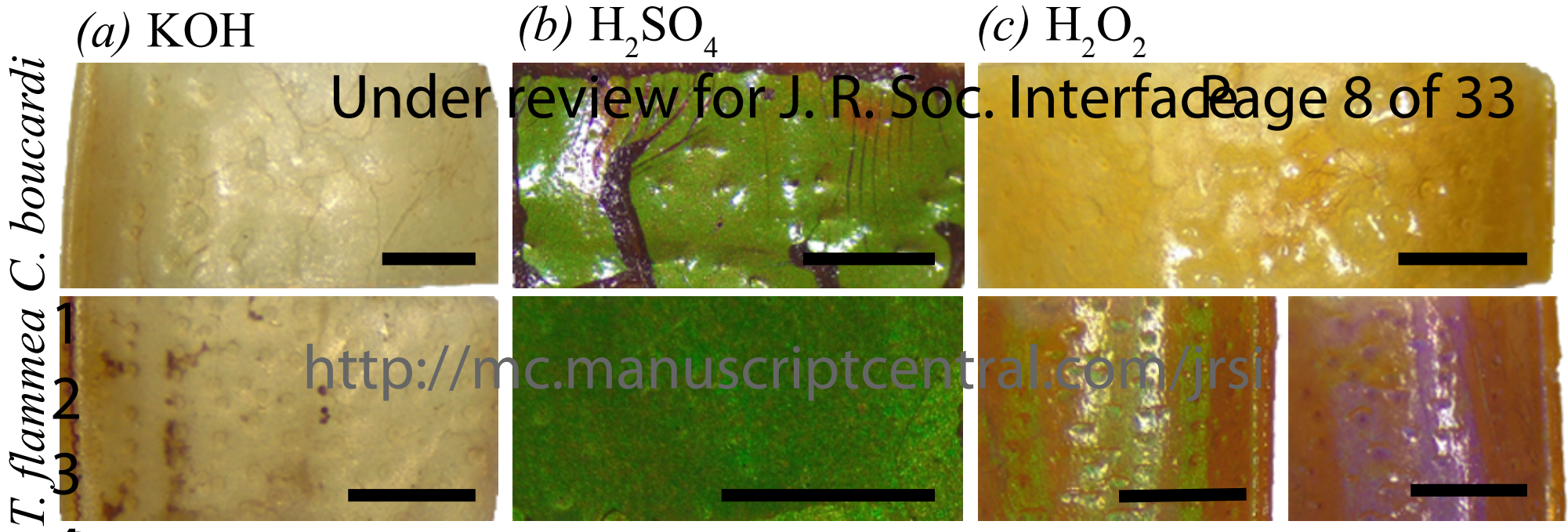

http://mc.manuscriptcentral.com/jrsi

SI Fig3

SI Figure 4

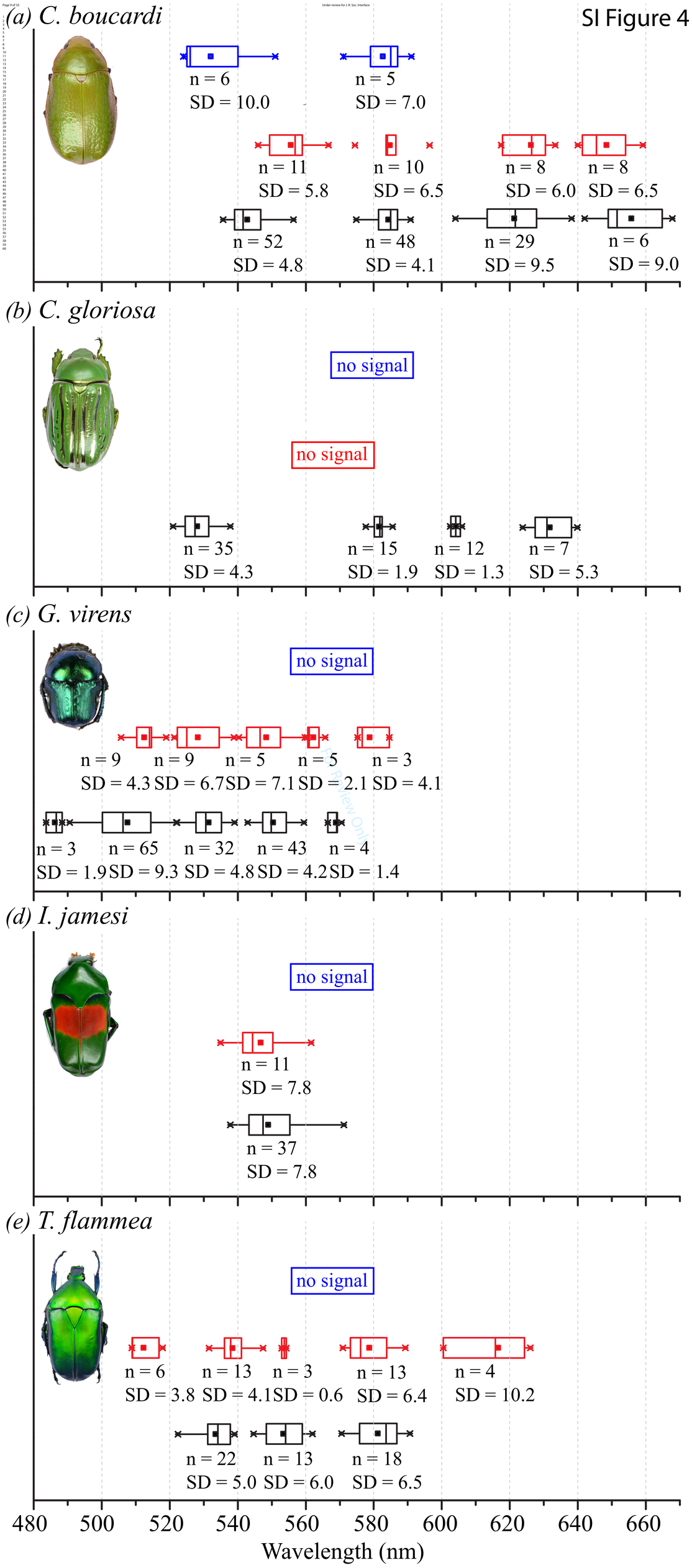

For Review Only

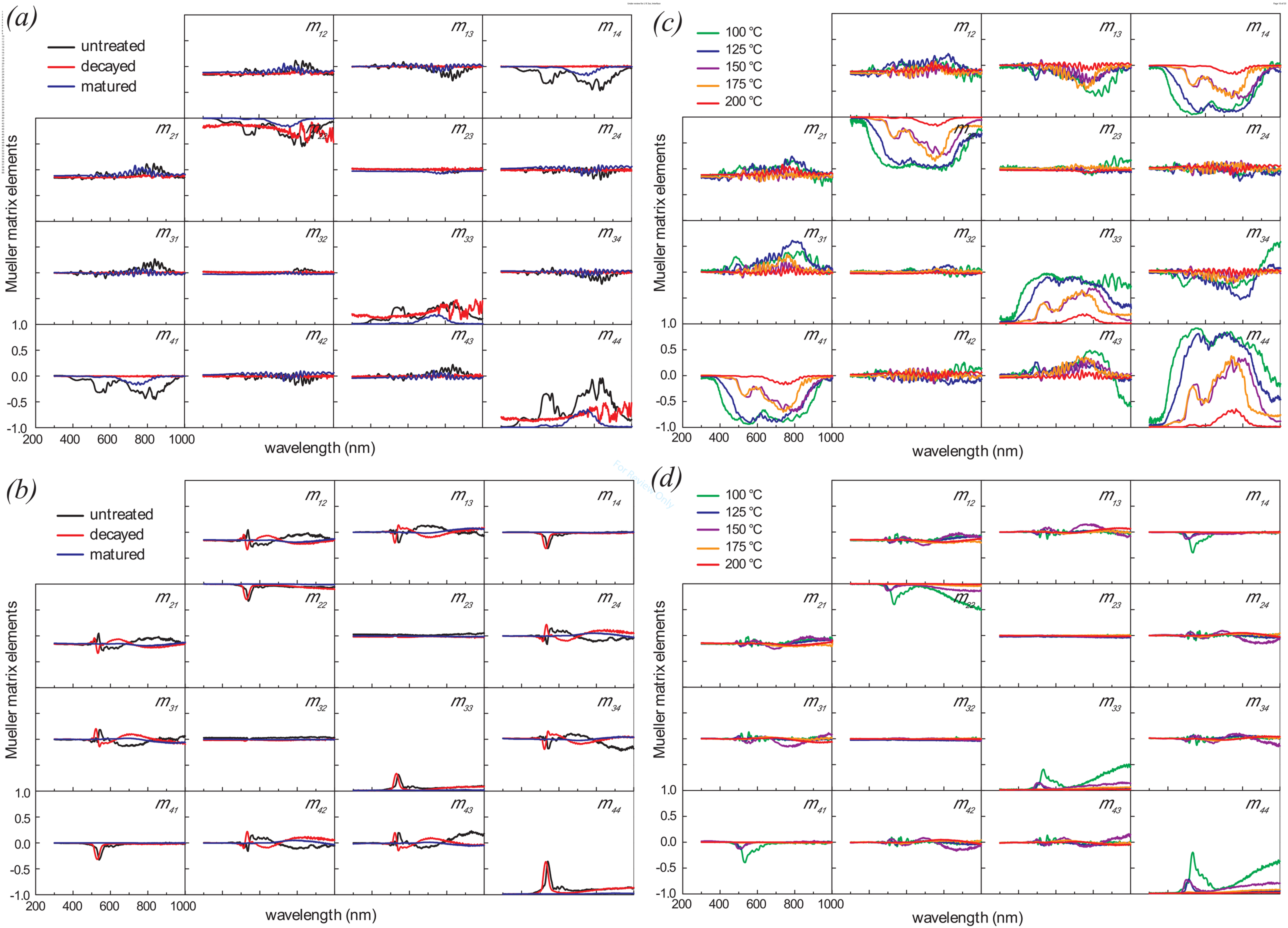
(a)
untreated
decayed
matured
(b)
untreated
decayed
matured
(c)
100 °C
125 °C
150 °C
175 °C
200 °C
(d)
100 °C
125 °C
150 °C
175 °C
200 °C
Mueller matrix elements
wavelength (nm)

SI Figure 5

Under review for J. R. Soc. Interface

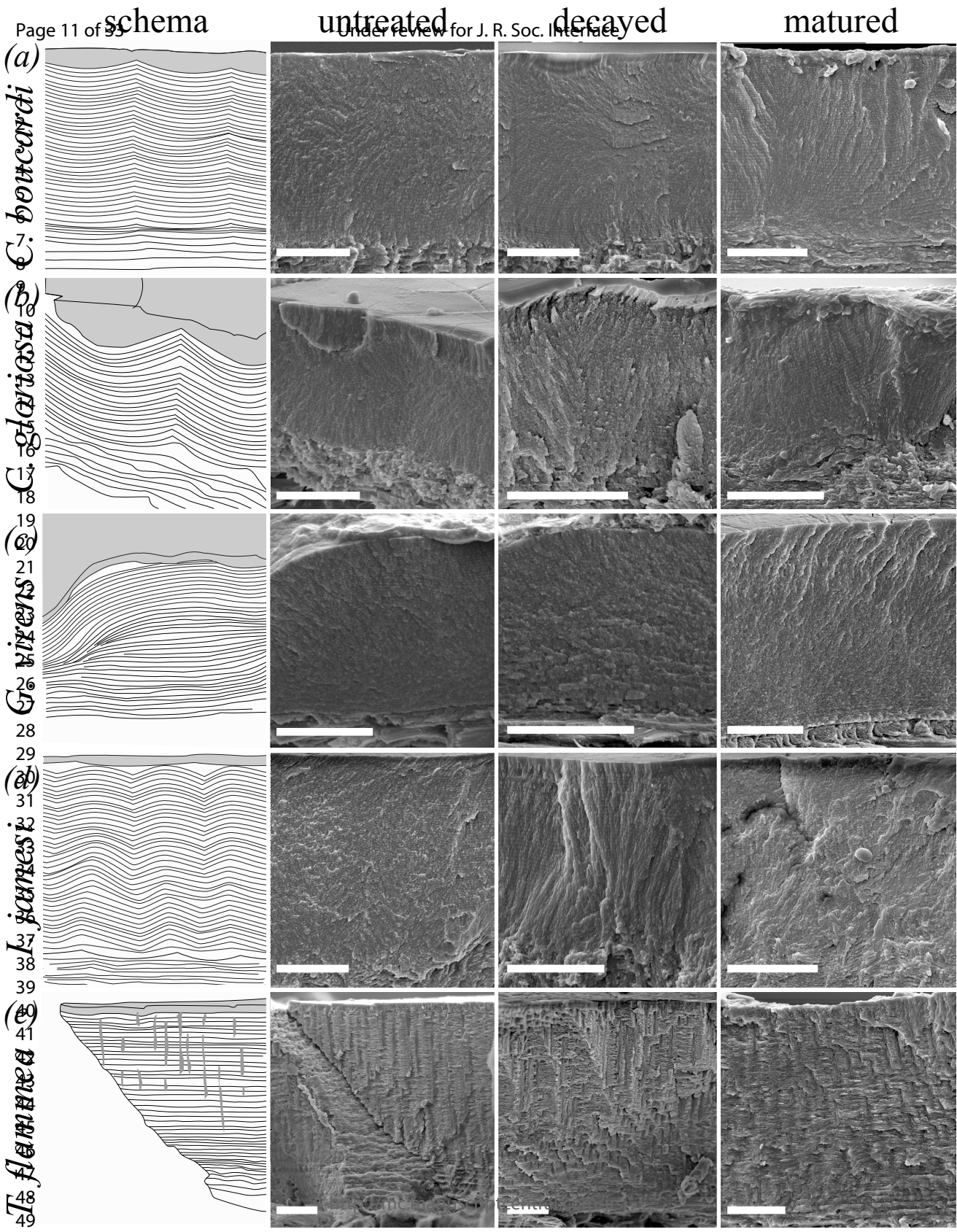

SI Figure 6

Experimental degradation of helicoidal photonic nanostructures in scarab beetles (Coleoptera: Scarabaeidae): implications for the identification of circularly polarizing cuticle in the fossil record

Giliane P. Odin[1*], Maria E. McNamara[1], Hans Arwin[2], Kenneth Järrendahl[2]

[1]School of Biological, Earth and Environmental Sciences, University College Cork, Distillery Fields, North Mall, Cork T23 TK30, Ireland; giliane.odin@gmail.com

[2]Department of Physics, Chemistry and Biology, Linköping University, SE-581 83 Linköping, Sweden

*Current address: Sorbonne Universités, UPMC, MNHN, CNRS, Centre de recherche sur la Paléobiodiversité et les Paléoenvironnements (CR2P) & Milieux environnementaux, transferts et interactions dans les hydrosystèmes et les sols (METIS), Paris, France

Abstract

Scarab beetles (Coleoptera: Scarabaeidae) can exhibit striking colours produced by pigments and/or nanostructures. The latter include helicoidal ('Bouligand') structures that can generate circularly polarized light, which have a cryptic evolutionary history in part because fossil examples are unknown. This suggests either a real biological signal, i.e., that Bouligand structures did not evolve until recently, or a taphonomic signal, i.e., that conditions during the fossilization process were not conducive to their preservation. We address this issue by experimentally degrading circularly-polarizing cuticle of modern scarab beetles to test the relative roles of decay, maturation and taxonomy in controlling preservation. The results reveal that Bouligand structures have the potential to survive fossilization, but preservation is controlled by taxonomy and the diagenetic history of specimens. Further, cuticle of specific genera (*Chrysina*) is particularly decay-prone in alkaline conditions; this may relate to the presence of specific compounds e. g. uric acid in the cuticle of these taxa.

Keywords

structural colours, Bouligand structure, taphonomy, fossil insects, Mueller-matrix ellipsometry

1. Introduction

The cuticle of insects is composed primarily of chitin microfibrilsembedded in a protein- and lipid-rich matrix, forming a multilaminate system [1]. These microfibrils constitute the bulk of the endo- and

For Review Only

exocuticle layers that provide rigidity to the exoskeleton and are covered by a lipid-rich epicuticle that forms a protective barrier and a sensory interface [2]. In the exocuticle, chitin microfibrils are usually mutually parallel in each layer [2, 3]. In some beetles, however, microfibrils of the outer exocuticle are slightly offset in successive layers, giving rise to helicoidal 'Bouligand' structures [4] that generate circularly polarized light (CPL; herein this term includes near-circular polarization) [2, 3].

Bouligand structures have been reported in plants [5], crustaceans [6] and beetles; the last of these includes eight genera of Scarabaeidae and one of Hybosoridae [7, 8].The biological significance of CPL is controversial, with much debate focussing on whether CPL functions in signalling(compare [9, 10] with [11] for behavioural studies) or is merely a by-product of the fibrillar and lamellar nature of the cuticle [12, 13].Recent discoveries of dedicated physiological characters for CPL detectionin the eyes of stomatopod crustaceans [14, 15, 16] support the hypothesis that CPL has important, albeit incompletely understood, biological functions.

Fossils have the potential to shed light on the functions and evolutionary history of CPL use in insects, providing Bouligand structures can be preserved. Fossil examples, however, have not been reported. This may reflect a real biological signal or an artefact of the fossilization process, i.e., reflecting poor preservation potential. This is a common issue in palaeobiological studies due to the incompleteness of the fossil record [17]. The two scenarios can, however, be discriminated with the aid of controlled laboratory experiments [18] designed to investigate the taphonomy of specific taxa, tissue structures, and/or biomolecules, thus informing on their preservation potential [19]. Previous taphonomic experiments investigating aspects of the fossilization process in various organisms, including arthropods, have identified a suite of factors which can influence the preservation potential of organisms (reviewed in [19, 20]). Known environmental factors include the extent of transport, relative timing of transport and decay, water temperature, salinity, pH, the presence of microbes, sediment type, sediment consistency, the availability of O_2 and mineral ions, and burial temperature and pressure. Biological factors include the nature and extent of decay, body geometry, and tissue composition. Clearly, not all potential factors can be investigated in a single experiment. Instead, rigorous taphonomic experiments typically investigate the impact of a small number of specific variables in a controlled manner (the 'reductionist' approach; [18]). In particular, previous taphonomic experiments have shed light on the preservational conditions and processes involved in the fossilization of multilayer reflectors and 3D photonic crystals in insects [21]. Here, we experimentally degraded extant scarab beetles with and without Bouligand structures in controlled laboratory decay and maturation experiments.

For Review Only

Untreated and degraded cuticles were analysed using scanning electron microscopy, reflectance microspectrophotometry and Mueller-matrix spectroscopic ellipsometry.

2. Material and methods

2.1 Material

Dried specimens of five green beetle taxa representing three sub-families of Scarabaeidae were procured from commercial suppliers: *Chrysina boucardi* (n = 3)and *Chrysina gloriosa* (n = 3) (both Rutelinae), *Ischiopsopha jamesi jamesi* (n = 3) and *Torynorrhina flammea flammea* (n = 3) (both Cetoniinae), and *Gymnopleurus virens* (n = 5) (Scarabaeinae).The cuticle of *T. flammea* does not generate CPL and served as a control; the cuticle of all other taxa used exhibits circular polarization [3, 22, 23, 24].

2.2 Light microscopy

Beetle elytra were imaged using a Leica DM2700M stereomicroscope coupled to a Leica MC190HD camera using unpolarized light from a LED lamp. Elytra were tested for circular polarization using a Nikon D3100 camera and a Leica EZ4W stereomicroscope equipped with left-handed and right-handed circular polarizers (EdmundOptics).

2.3 Scanning electron microscopy

Samples of elytra were mounted on aluminium stubs using carbon tape, sputter-coated with Au/Pd and examined using an FEI Inspect F50FE-SEM and an FEI Quanta 650 FE-SEM at 5 kV in secondary electron mode.

The period of the helicoidal structure, called pitch (p), corresponds to a full turn (360 °) of the chitin fibrils and consists of two successive lamellae (thickness α), i.e., $p=2\alpha$. The lamellar thicknesses were obtained from SEM images (see below) using the FFT (Fast Fourier Transform) function in Image J [25].

2.4 Microspectrophotometry

Reflectance spectra were collected on elytra with a Zeiss Axioskop 2 microscope using the x50 objective and equipped with a halogen lamp (HAL 100) set to 6V and an Ocean Optics USB4000 spectrometer. Specimens were manually positioned so that the region to be analysed was approximately at normal incidence to the light path. Acquisition time varied from 5–10 s. Between three and five replicates were

For Review Only

used for each sample. Data were normalized relative to a white standard (Certified Reflectance Standard, Labsphere) and analyzed using Ocean Optics SpectraSuite software. Models of the theoretical wavelengths produced from the exocuticular lamination were based on the circular Bragg's equation for normally incident light $\lambda_{max} = pn_{av} = 2\alpha n_{av}$ where λ_{max} is the wavelength at the circular Bragg peak and n_{av} is the average of the two refractive indices in the anisotropic lamellae plane. In this study we neglect dispersion and use n_{av}= 1.56 [26].

2.5 Mueller matrix spectrometric ellipsometry

Normalized Mueller matrices of cuticle samples were measured with a dual rotating compensator ellipsometer (RC2, J. A. Woollam Co., Inc.) at an angle of incidence of 20°. Focusing probes were used to obtain a spot size of less than 100 µm. The Mueller matrices presented here are primary data without any filtering or data processing. Further technical details and limitations are reported in [27].

2.6 Decay experiments

Experiments were designed to approximate decay of insect cuticles in still aqueous environments as most fossil insects are from ancient lacustrine sediments [28]. We considered the following variables: temperature, pH, microbes and sediment. Water temperature is a major control on preservation as it controls the rate of decay [29]. We conducted our experiments at 30 °C to promote decay and delivery of useful results within the project timeframe (even though benthic waters can be much cooler than this in many extant lakes).Our experiments used an alkaline pH as insect cuticles decay slightly faster in such media than in acidic media (McNamara, unpub. data). Although previous experiments have demonstrated that decay is enhanced in the presence of sediment [30], even particular clay minerals [31], and in the presence of an external source of microbes [30] (i.e. not those in / on the carcass itself), we conducted our experiments using distilled water without inocula of sediment and bacteria in order to mitigate against occlusion of the cuticle surface by sedimentary particles and / or a microbial biofilm. Small fragments of elytra (ca. 5 x 5 mm^2; n = 3 for each taxon) were immersed in individual glass vials each filled with 10 mL of water at pH 11.5 +/-0.1 and degraded for three months in a controlled temperature chamber at 30 °C (+/- 1 °C) in the dark. The pH of the decay media was measured at the start and termination of the experiments. In order to track short-term changes in visible colour, additional specimens of *C. gloriosa* and *C. boucardi* were degraded in identical conditions to those described above and photographed at two-week intervals for three months.

For Review Only

2.7 High-temperature maturation experiments

Small fragments of untreated elytron (ca.5 x 5 mm^2) were wrapped in aluminium foil and matured at one of each of the following conditions for 24 h at 1 bar: 95 °C, 100 °C, 125 °C, 150 °C, 175 °C, 200 °C.

2.8 Chemical tests

A series of supplementary experiments investigated the impact of other factors on the preservation of Bouligand structures, using techniques that have been applied to studies of the origins of structural colour in other taxa [32]. In particular, we carried out tests designed to reveal which cuticle layer(s) are involved in production of the visible hue, and whether the observed hue is entirely structural or includes a pigmentary component. Small fragments of untreated elytra from *C. boucardi* and *T. flammea* were treated in the following ways: immersion in (i) 8 % KOH (60 °C, 1 bar, 24 h; to remove the epicuticle [32]), (ii) 10 % H_2O_2 (60 °C, 1 bar, 24 h; to remove the procuticular layers [32]), (iii) 20 % H_2SO_4 (20 °C, 1 bar, 24 h; to bleach melanin [32]), and (iv) wrapped in polytetrafluoroethylene (PTFE; 200 °C, 1 bar, 24 h) to simulate maturation in anoxic conditions. To test the influence of the aluminium foil upon maturation, some cuticle samples were also matured without being wrapped and placed in a glass petri dish. The results were assessed qualitatively via visual inspection of cuticle after treatment.

Untreated cuticle samples were also immersed in methyl salicylate (refractive index 1.54) to test whether the observed colour is structural [33].

3. Results

3.1 Visible hue

The visible hue has been investigated by eye and light microscopy. Untreated cuticle in all taxa is highly reflective and exhibits a bright green colour (**figure 1***a–e*) that in *C. gloriosa* is combined with golden stripes in (**figure 1***b*) and in *I. jamesi* red regions (**figure 1***d*).

Colour did not change during decay of *G. virens*, *I. jamesi* and *T. flammea* (**figure 1***c–e*). During decay of *C. gloriosa* and *C. boucardi*, however, colour altered from green to red-orange (**figure 2***a*), and ultimately to a matte dark brown (**figure 1***a,b)*; the region of *C. boucardi* cuticle that remained green after decay has not been in contact with the decay medium (**figure 1***a*). Alteration initiated on the golden stripes of *C. gloriosa* and extended progressively to the green cuticle regions. In contrast, alteration of hue in *C. boucardi* initiated at cut edges and cuticular pores (see S.I.**figure 1**).

For Review Only

All cuticle samples were altered to black during maturation, both in the presence (**figure 1***a–e*) and absence of oxygen (S.I. **figure 2***a*) except for *C. boucardi* which altered into a dark green colour (**figure 1***a*).Wrapping cuticle in aluminium foil does not influence the results (S.I. **figure 2***b*).

The supplementary experiments reveal that the green hue of the cuticle in all taxa is less intense after H_2SO_4 treatment and is lost upon treatment with KOH (S.I. **figure 3**). Treatment with H_2O_2 resulted in loss of visible colour in *C. boucardi* and reduction in intensity plus a blue shift in hue in *T. flammea*.

3.2 Surface texture

The surface texture has been investigated using both light and electron microscopies. Green cuticle regions in *C. boucardi*, *C. gloriosa*, *I. jamesi* and *T. flammea* exhibit a tessellated surface pattern defined by a combination of pentagonal, hexagonal and heptagonal units 7–10 µm wide (**figure 2***a,b,d,e*). In *C. boucardi* and *C. gloriosa*, the units are green with yellow cores (**figure 2***a,b*),those in *I. jamesi* are green throughout (**figure 2***d*) and those of *T. flammea* are green-blue throughout (**figure 2**e).These tessellated surface patterns are superimposed onto taxon-specific microtextures, as evidenced by SEM micrographs. In *C. gloriosa*, green (but not gold-coloured) regions exhibit a stellate pattern comprising a series of star-shaped units each ca. 5 µm wide (**figure 2***b*). In *I. jamesi*, the elytral surface texture (both green and red regions) is dominated by near-parallel rows of elongate projections, each ca. 5 µm long (**figure 2***d*). *T. flammea* exhibits a reticulate structure, with alveoli ca. 10 µm wide, sometimes with a dark central spot (**figure 2***e*). A similar, but subtler, structure is present in *C. boucardi* (**figure 2***a*). *G. virens* elytra do not exhibit surface patterns or microtextures (**figure 2***c*).

After decay, brown regions of *C. boucardi* and *C. gloriosa* cuticle retain a tessellated surface texture but the polygonal units no longer differ in hue between core and margins (**figure 2***a,b*). SEM analysis reveals that the green regions of degraded *C. boucardi* cuticle exhibit surface microtextures that are identical to those in untreated cuticle (**figure 2***a*). Brown cuticle regions show surface pitting (**figure 2***a*). The surface microtextures of *C. gloriosa* are clearly altered during decay, via expansion of the star-shaped units and loss of surface cohesion (**figure 2***b*). Finally, decay does not affect the visible colour and surface microtexture of *G. virens*, *I. jamesi* and *T. flammea* (**figure 2***c–e*).

Following maturation, all taxa retain surface microtextures despite loss of visible colour (**figure 2***a–e*).

For Review Only

3.3 Reflectance microspectrophotometry

Reflectance spectra (**figure 3** and S.I. **figure 4**) are consistent with the observations on visible hue described above. In *C. boucardi* (**figure 3***a*), untreated cuticle samples display two primary peaks at ca. 545 and 585 nm, plus secondary peaks (up to three) between 605 and 675 nm; after decay, spectra of green cuticle regions change slightly (the primary peak at 545 nm shifts to 555 nm) while spectra from brown cuticle regions lack peaks. After maturation, cuticle exhibits a single broad peak centred on 530 nm and a secondary peak at 585 nm.

In *C. gloriosa* (**figure 3***b*), spectra of untreated cuticle samples exhibit a primary peak at ca. 530 nm with secondary peaks at 580 nm, 605 nm and 630 nm. Spectra of decayed and matured cuticle lack peaks.

Specimens of *G. virens* vary markedly in spectral characteristics among specimens. In four specimens, spectra of untreated cuticle usually exhibit two primary reflectance peaks at 485–520 nm and 530–570 nm. The remaining two specimens, however, show three peaks at ca. 500 nm, 530 nm and 555 nm (**figure 3***c*). In all specimens, decay resulted in a shift of these peaks towards longer wavelengths; spectra of matured cuticle lack peaks.

Spectra of untreated *I. jamesi* cuticle show one primary peak at ca. 550 nm and, sometimes, a secondary peak at ca. 635 nm for male specimens or 605 nm for females (**figure 3***d*). Decay did not result in major spectral changes (peak position shifted by ± 5 nm); spectra of matured cuticle lack peaks.

Finally, spectra from *T. flammea* cuticle can exhibit one, two or three peaks at 535 nm, 555 nm and 580 nm (**figure 3***e*). Decay results in minimal shift of these peaks (± 5 nm) and the appearance of additional major peaks at 510 nm and 615 nm. Spectra of matured cuticle lack peaks.

In general our spectrophotometric data correspond well to the measured data; the slight discrepancy between both datasets may originate from a slight deviation of the cuticle surface from normal during spectrophotometric analysis, or from the value of the refractive index used.

3.4 Polarization analysis

Polarization has been analysed qualitatively through circular polarizers attached to visualisation systems (camera and stereomicroscope), and quantitatively by Mueller matrix spectrometric ellipsometry. All CPL-producing taxa studied exhibit a green colour when observed using the left-handed circular polarizer but a brown colour when observed using the right-handed circular polarizer, confirming reflection of left-handed polarized light (**figure 1***a*–*d*). The brown (not black) colour indicates some

For Review Only

reflected broadband CPL. These effects are apparent in cuticle regions of all colours and from all body regions; the structures responsible for circular polarization are thus ubiquitous and independent of visible hue. *T. flammea* appears green when observed using each polarizer, confirming its optical inactivity (**figure 1***e*).

Circular polarization is retained where original cuticle colour persists during decay (observed in *G. virens*, *I. jamesi* and *T. flammea*; **figure 1***c–e*). Visual assessment of polarizationis not possible where visible hue altered from green to matte brown (as for decayed cuticle; **figure 1***a,b*) or black (as for matured cuticle; **figure 1***a–e*).

These results are confirmed and explored further by Mueller matrix analysis on cuticle samples from *C. boucardi* and *I. jamesi*. **Figure 4** presents the Mueller matrix element m_{41}, which is non-zero if the light has a circularly polarized component (the full Mueller matrices are presented in **S.I. figure 5**). The negative values obtained on m_{41} verify that left-handed CPL is reflected. The m_{41} obtained on untreated cuticle of *C. boucardi* exhibits two major spectral bands centred around 550 nm and 800 nm corresponding to reflection of green and red/infrared CPL, respectively (**figure 4***a*). For *I. jamesi*, a single narrow spectral band is obtained around 540 nm (**figure 4***b*). The effect of decay and maturation is detailed in **figure 4***a* and **4***b*. On the brown-coloured decayed cuticle of*C. boucardi*, the Mueller matrices lack features in all the off-diagonal block elements (**S.I. figure 5***a*), including the m_{41} where the signal disappears (**figure 4***a*). In contrast, left-handed polarized light is reflected from decayed cuticle that retain a green hue (**figure 4***b*; *I. jamesi*). A blue-shift of the m_{41} feature from 540 nm to 529 nm is, however, visible.

The maturation process has similar effects on *I. jamesi* and *C. boucardi* whereby loss of colour is accompanied by a weakening of the circular polarization, up to its loss for *I. jamesi* (**figure 4***a*,*b*).

Figures 4*c* and **4***d* show the effect of thermal treatment during maturation: the m_{41} signal becomes less negative with increasing temperature, approaching zero at 200 °C for *C. boucardi* and 175 °C for *I. jamesi*, whereby the circular polarization is lost. For *C. boucardi*, the green reflection band is more susceptible to alteration than the red/infrared: it is altered at lower temperature relative to the red/infrared band and indicates a colour shift from green to red/brown. At 200 °C, while the visible contribution has disappeared, the red/infrared band is still present. For *I. jamesi*, a small blue shift occurs along with increasing temperature before the production of a flat signal.

For Review Only

3.5 SEM of vertical cross sections

All CPL-producing beetle cuticle samples exhibit a thin homogenous superficial epicuticle underlain by a thinly laminated exocuticle and, in turn, by a thicker endocuticle comprising a cross-ply arrangement of bundles of chitin microfibrils (**figure 5** and **S.I.figure 6**). Except for *G. virens*, the exocuticle is subdivided into outer and inner regions with thin, and thick, lamellae, respectively. This subdivision is not apparent in the non CPL-producing cuticle of *T. flammea*, but striking vertical structures are present (**figure 5***e* and S.I. **figure 6***e*).The dimensions of various cuticular components are summarized in **table 1**.

The morphology of the lamellae in the outer exocuticule varies markedly among specimens. Lamellae form distinctive concentric cusps 7–10 µm wide (each centred on the surficial 'star' of the texture) in the green cuticular regions of both *Chrysina* species (**figure 5***a,b* and S.I. **figure 6***a,b*). Lamellae are flat and parallel to the cuticle surfacein *G. virens* (**figure 5***c* and S.I. **figure 6***c*), *T. flammea* (**figure 5***e* and S.I. **figure 6***e*) and gold regions of *C. gloriosa,* and undulose in *I. jamesi* (**figure 5***d* and S.I. **figure 6***d*). Lamellae are flat and parallel to the surface in the inner exocuticle of all taxa (S.I. **figure 6**).

Decay does not alter the morphology of the exocuticular lamellae but reduces the thickness of the latter in *C. boucardi* and *C. gloriosa* by 48 % and 49 %, respectively (**table 1**). In contrast, maturation results in a less marked reduction in lamella thicknessin all taxa (6–14 %).

4. Discussion

4.1 Source of visible colour

We examined multiple specimens of each of the extant taxa studied in order to assess the extent of any intraspecific variations in colour (common in extant beetles, e.g. *T. flammea* [24], *Cetonia aurata* [34] and *Plateumaris sericea* [35]). Our reflectance data on the green cuticle regions are consistent with previously reported λ_{max} values for *C. gloriosa* (530 and 580 nm [36]), *C. boucardi* (519, 588 and 620 nm [22]) and *T. flammea* (490, 530, 568 and 584 nm [24]). These spectroscopic data, plus those for *I. jamesi* and *G. virens*, are consistent with our models of the theoretical wavelengths (**table 2**): observed and predicted λ_{max} values differ by only 0.3–6.8 % across taxa, supporting that the visible colour is primarily structural.

Immersion of structurally coloured materials in a medium of similar refractive index as the chitin matrix results in loss of iridescence; this has been considered a proxy for structural colour [33]. Immersion of cuticle from *C. boucardi* in methyl salicycliate (with a refractive index of 1.54 close to chitin 1.56) does not affect the observed hue, suggesting that the visible colour results from a combination of structural colour (i.e., generated by the Bouligand structure) plus pigment i.e, melanin. This is consistent

For Review Only

with our experimental evidence for melanin in the cuticle (i.e., a reduction in the intensity of the observed colour upon treatment with H_2O_2) and with studies of *C. boucardi* where a contribution from melanin is required for consistency between experimental and theoretical models of visible colour [22].

Finally, the supplementary experiments demonstrated that the epicuticle, but not the endocuticle, is also involved in the production of visible colour. The role of the former may relate to scattering of light from epicuticular lipids [37].

4.2 Origins of colour changes during taphonomic experiments

Structural colours in scarabs have been attributed to constructive interference produced by highly regular spacing of lamellae in the exocuticle [3]. The colour reflected depends on the periodicity of the structure and its refractive index [3] [26] while its brightness and purity relate (among other factors) to the order of the structures and the thickness of the colour and CPL-generating stack [26]. Based on the lamellar thickness in decayed cuticle and using a refractive index of 1.56 for chitin, *C. boucardi* and *C. gloriosa* should exhibit λ_{max} in the UV part of the spectrum (λ_{max}= 296 nm for *C. bourcardi*, λ_{max}= 343 nm for *C. gloriosa*). Similarly, after maturation, lamellar thickness predicts that samples should exhibit λ_{max} in the blue-green to green-yellow regions of the visible spectrum (λ_{max} = 544 nm for *C. boucardi,* 561 nm for *C. gloriosa,*484 nm for *I. jamesi*, 515 nm for *G. virens* and 577 nm for *T. flammea*). Instead, in all cases, the cuticle is brown and their reflectance spectra lack peaks (in the visible range).

In brown decayed cuticle, the thickness of exocuticular lamellae is clearly altered and the structural colour contribution shifts toward shorter wavelengths in the UV part of the spectrum. The brown colour displayed by decayed cuticle must therefore relate to the presence of melanin (see above), which commonly functions as a light-absorbing layer in photonic nanostructures [37].

For matured cuticle, there is no evidence for striking changes in the thickness or regularity of exocuticular laminae. This suggests that the colour change (to black) in the experimentally matured beetles is chemical rather than structural in origin. The supplementary experiments demonstrate that the preservation potential of the cuticle is independent of ambient oxygen levels. Critically, our experiments demonstrate that preservation of colour is subject to a strong temperature control: colour survives below, but not above, 150 °C. Colour change is thus unlikely to indicate marked dehydration (as in the scarab *Dynastes hercules* [38]) since cuticle does not change in visible colour after experimental maturation for 24 h at 95 °C, 105 °C or 125 °C. Rather, these data suggest that colour changes during maturation most likely relate to polymerization, which is typical of maturation (but initiates during decay) [39]. Notably, polymerization alters the refractive index of the cuticle, which affects the

For Review Only

absorbance windows, thus controlling the visible colour produced. This process has been reported from other experimentally degraded structurally coloured insect cuticle [21].

Combined, these results suggest that preservation of Bouligand structures in fossils is controlled by diagenetic history, in particular, the maximum burial temperatures of the host sediment.

4.3 Changes in polarisation during experiment

All CPL-producing taxa studied reflect left-handed polarized light, which is consistent with previous studies [3, 8, 22, 36, 40]. In most elements, oscillations are observed. These are due to interference effects in various parts of the cuticle and can in some cases be used to determine pitch profiles and cuticle internal dimensions, as shown in [41].

Our data demonstrate a strong relationship between either loss or survival of visual colour and polarization upon degradation. Typically, the features observed on the decayed cuticle of *C. boucardi* indicate that the cuticle is a dielectric material, e.g. like a plastic surface, reflecting light as an isotropic material without any active Bouligand structure or other anisotropic features. Moreover, the ellipsometry data recorded on matured cuticle confirm that the optical effect of Bouligand structures is indeed destroyed during maturation, and not shifted toward wavelengths outside the visible spectral range, despite survival of the Bouligand structure itself (**figure 5**). The loss of the CPL effect may rather be due to chemical alteration causing a major change in refractive index or increased near-surface absorption preventing the light from interacting with the Bouligand structures.

The shift in the circular polarization signal differs between taxa. Since the structures responsible for CPL are indeed preserved (**figure 5** and **S.I. figure 6**), these differences likely reflect a difference in chemistry between *C. boucardi* and *I. jamesi*.

4.4 Taxonomic controls on fossilization

The preservation potential of insects in the fossil record is influenced by body size, morphology and the hardness of the cuticle [42, 43, 44]. Small and robust beetles, and their more sclerotized body parts, e.g. elytra, are more likely to be preserved [43, 45, 46, 47]. The cuticle of scarabs is one of the most robust among insects [43]; preservation of Bouligand structures in fossil scarabs does not, therefore, appear unlikely.

Our study reveals a strong taxonomic control on the preservation of visual colour and polarization properties of Bouligand structures during experimental decay, whereby the response of *Chrysina* cuticle differs to that of all other taxa studied. This contrasts with the taphonomy of multilayer reflectors, which

For Review Only

is independent of taxonomy [33]. *C. boucardi* and *C. gloriosa* differ in their ecology to the other taxa studied here: *Chrysina* species are nocturnal and feed on foliage whereas the other taxa are diurnal and feed on dung (*G. virens*) or on flowers and fruits (*I. jamesi* and *T. flammea*). These parameters are unlikely to relate to the preservation of Bouligand structures. The exocuticular laminae in green cuticle regions of the studied *Chrysina* shows a distinctive cuspate arrangement (see [48]), but it is unclear how this physical structure could relate to preservation of Bouligand structures. Finally, experimental degradation does not alter the structure of the exocuticular laminae in any taxon studied.

Instead, the taxonomic signal most likely reflects chemical alteration of the cuticle. Variations in chitin chemistry is unlikely to be a factor as the cuticle of all arthropods comprises α-chitin [49] and degrades thermally only above 300 °C [50]. Given the contribution of the lipid-rich epicuticle and of melanin to visible colour in the taxa studied (see above), it is possible that such cuticular components could chemically alter during the experiments, thus changing the refractive index of the cuticle. Indeed, epicuticular lipids are sensitive to basic treatment (similar to our decay experiments [32]) and are known to vary in composition among taxa [51]; the cuticular lipid inventory (see review in [52]) and pigment chemistry (see review in [53]) of the taxa studied here have not, however, been characterized, so we cannot assess whether these indices contribute to the observed taxonomic signal.

The studied taxa do, however, vary in other aspects of cuticle chemistry, notably the presence / absence of uric acid, which increases refractive index and enhances the birefringence of the chitin-matrix [54], thus resulting in more efficient reflection of incoming light. The taxonomic distribution of uric acid in insect cuticle has been investigated only in a single study in which uric acid was reported from three *Chrysina* species but not in the only non-*Chrysina* genus (*Potosia speciossima)* examined [54]. In living insects, theacidic physiological pH [55] implies that uric acid is present in the acid form ($C_5H_2N_4O_3H_2$). At high pH (as in our decay experiments), however, uric acid exists as $C_5H_2N_4O_3^{2-}$. The impact of this chemical change on the optical properties of cuticle is unknown. It is therefore not implausible that the loss of visible colour and polarization in *Chrysina* cuticle during decay may reflect the degradation of uric acid to urate or other chemical compound.

These results may have broader applications in the fossil record, suggesting the presence of a taphonomic bias related to taxon-specific cuticle chemistry. While acidic environments have been hypothesized to promote chitin degradation through hydrolysis [56], we hypothesise that cuticle rich in uric acid will be relatively susceptible to degradation in alkaline conditions. Fossil insect biotas preserved in sediments that have experienced relatively alkaline conditions during decay may thus be biased towards taxa without cuticular uric acid; this bias may be less pronounced in biotas that experienced

For Review Only

relatively milder conditions. Future experimental studies will characterize more fully the impact of uric acid on the taphonomy of cuticle in diverse insect taxa.

5. Conclusion

This work is the first study investigating the preservation of Bouligand structures in insects. Our results demonstrate that Bouligand structures can survive decay and maturation and thus have the potential to be fossilized. Future analyses of fossil insects preserving structural colours should therefore test for ultrastructural evidence for Bouligand structures. The presence of strong temperature-related control on preservation suggests that the fossil record of Bouligand structures may be biased, whereby preservation is more likely for cuticle subjected to lower temperatures during diagenesis. This may belie a broader taphonomic bias relating to the nature of epicuticular lipids and / or pigments (e.g. melanin) and / or the concentration of uric acid, whereby insects with cuticle that contain uric acid may be less likely to survive decay in alkaline conditions than cuticle lacking uric acid. These hypotheses can be tested by future experimental investigations and analyses of fossil insects preserving structural colours should test for ultrastructural evidence of Bouligand structures. Additionally, geochemical studies should incorporate data on the diagenetic history of the host sediment. This will help to constrain fossil localities where Bouligand structures are more likely to be preserved. Additionally, such results have broader implications in the field of bio-inspired photonic materials, whereby the stability of Bouligand structures during thermal treatment can be of interest for banknote sensors (anti-counterfeiting) or light-emitting sources (screen technology).

Acknowledgments

We thank Luke McDonald, Martin Pemble, Tomas Kohoutek and Mikhail Parchine for useful discussions. G.P.O. is grateful to J. David Pye for access to unpublished data. The research is funded by Science Foundation Ireland ERC Support Grant SFI 16/ERCS/3904 and European Research Council Starting Grant H2020-2014-StG-637691-ANICOLEVO awarded to M.E.M.

Author's contributions

M.E.M. and G.P.O. designed the research. H.A. and K.J. performed Mueller-matrix analysis and G.P.O. conducted all other analyses. G.P.O. and M.E.M. interpreted results and wrote the manuscript with contributions from all other authors.

For Review Only

Data availability

The data are publically available on CORA (https://cora.ucc.ie/handle/10468/6491).

Competing interests

The authors declare no competing interests.

References

[1] Chapman RF; 2013. Chapter 16: Integument. In: Douglas SJSAE, editor. The insects: Structure and function. Cambridge University Press. p. 463–500.

[2] Neville AC; 1975. Chapter 2: General structure of integument. In: Biology of the Arthropod Cuticle. Springer. p. 7–70.

[3] Neville AC, Caveney S. 1969. Scarabaeid beetle exocuticle as an optical analogue of cholesteric liquid crystals. Biological Reviews. 44, 531–562. doi:10.1111/j.1469-185X.1969.tb00611.x.

[4] Bouligand Y. 1965. Sur une architecture torsadée répandue dans de nombreuses cuticules d'Arthropodes. Comptes Rendus Hebdomadaires des Séances de l'Académie des Sciences de Paris. 261, 3665–3668.

[5] Vignolini S, Moyroud E, Glover BJ, Steiner U. 2013. Analysing photonic structures in plants. Journal of The Royal Society Interface. 10, 9. doi:10.1098/rsif.2013.0394.

[6] Neville AC, Luke BM. 1971. Form optical activity in crustacean cuticle. Journal of Insect Physiology. 17, 519–526. doi:10.1016/0022-1910(71)90030-8.

[7] Michelson AA. 1911. On metallic colouring in birds and insects. The London, Edinburgh, and Dublin Philosophical Magazine and Journal of Science. 21, 554–567. doi:10.1080/14786440408637061.

[8] Pye JD. 2010. The distribution of circularly polarized light reflection in the Scarabaeoidea (Coleoptera). Biological Journal of the Linnean Society. 100, 585–596. doi:10.1111/j.1095-8312.2010.01449.x.

[9] Brady P, Cummings M. 2010. Differential response to circularly polarized light by the jewel scarab beetle *Chrysina gloriosa*. The American Naturalist. 175, 614–620. doi:10.1086/651593.

[10] Warrant EJ. 2010. Polarisation vision: beetles see circularly polarised light. Current Biology. 20, R610–R612. doi:10.1016/j.cub.2010.05.036.

For Review Only

[11] Blahó M, Egri A, Hegedüs R, Jósvai J, Tóth M, Kertész K, et al. 2012. No evidence for behavioral responses to circularly polarized light in four scarab beetle species with circularly polarizing exocuticle. Physiology & Behavior. 105, 1067–1075. doi:10.1016/j.physbeh.2011.11.020.

[12] Neville AC; 1975. Chapter 8: Physical properties. In: Biology of the arthropod cuticle. Springer. p. 319–374.

[13] Cronin TW, Shashar N, Caldwell RL, Marshall J, Cheroske AG, Chiou TH. 2003. Polarization vision and its role in biological signaling. Integrative and Comparative Biology. 43, 549–558. doi:10.1093/icb/43.4.549.

[14] Chiou TH, Kleinlogel S, Cronin T, Caldwell R, Loeffler B, Siddiqi A, et al. 2008. Circular polarization vision in a stomatopod crustacean. Current Biology. 18, 429–434. doi:10.1016/j.cub.2008.02.066.

[15] Gagnon Y, Templin R, How M, Marshall NJ. 2015. Circularly polarized light as a communication signal in mantis shrimps. Current Biology. 25, 3074–3078. doi:10.1016/j.cub.2015.10.047.

[16] Templin RM, How MJ, Roberts NW, Chiou TH, Marshall J. 2017. Circularly polarized light detection in stomatopod crustaceans: a comparison of photoreceptors and possible function in six species. Journal of Experimental Biology. 220, 3222–3230. doi:10.1242/jeb.162941.

[17] Briggs DEG. 2003. The role of decay and mineralization in the preservation of soft-bodied fossils. Annual Review of Earth and Planetary Sciences. 31, 275–301. doi:10.1146/annurev.earth.31.100901.144746.

[18] Purnell MA, Donoghue PJC, Gabbott SE, McNamara ME, Murdock DJE, Sansom RS, et al. Experimental analysis of soft-tissue fossilization: opening the black box. Palaeontology. 61, 317–323. doi:10.1111/pala.12360.

[19] Briggs DEG, McMahon S, Smith A. 2016. The role of experiments in investigating the taphonomy of exceptional preservation. Palaeontology. 59, 1–11. doi:10.1111/pala.12219.

[20] Gupta NS, Briggs DEG; 2011. Taphonomy of animal organic skeletons through time. In: Springer, editor. Taphonomy: Process and Bias Through Time. p. 199–221.

[21] McNamara ME, Briggs DEG, Orr PJ, Gupta NS, Locatelli ER, Qiu L, et al. 2013. The fossil record of insect color illuminated by maturation experiments. Geology. 41, 487–490. doi:10.1130/G33836.1.

[22] Jewell SA, Vukusic P, Roberts NW. 2007. Circularly polarized colour reflection from helicoidal structures in the beetle *Plusiotis boucardi*. New Journal of Physics. 9, 99.

[23] Agez G, Bayon C, Mitov M. 2017. Multiwavelength micromirrors in the cuticle of scarab beetle *Chrysina gloriosa*. Acta Biomaterialia. 48, 357–367. doi:10.1016/j.actbio.2016.11.033.

For Review Only

[24] Song CX, Liu F, Hao YH, Hu XH, Zhang YF, Liu XH. 2014. Multilayer manipulated diffraction in flower beetles *Torynorrhina flammea*: intraspecific structural colouration variation. Journal of Optics. 16, 105302.

[25] Schneider CA, Rasband WS, Eliceiri KW. 2012. NIH Image to ImageJ: 25 years of image analysis. Nature methods. 9, 671–675.

[26] Land MF. 1972. The physics and biology of animal reflectors. Progress in Biophysics and Molecular Biology. 24, 75 – 106. doi:10.1016/0079-6107(72)90004-1.

[27] Arwin H, Berlind T, Johs B, Järrendahl K. 2013. Cuticle structure of the scarab beetle *Cetonia aurata* analyzed by regression analysis of Mueller-matrix ellipsometric data. Optics Express. 21, 22645–22656. doi:10.1364/OE.21.022645.

[28] Grimaldi D, Engel MS. 2005. Evolution of the Insects. Cambridge University Press.

[29] Kidwell SM, Baumiller T. 1990. Experimental disintegration of regular echinoids: roles of temperature, oxygen, and decay thresholds. Paleobiology. 16, 247–271.

[30] Briggs DEG, Kear AJ. 1993. Decay and preservation of polychaetes: taphonomic thresholds in soft-bodied organisms. Paleobiology. 19, 107–135. doi:10.1017/S0094837300012343.

[31] Murdock DJE, Gabbott SE, Mayer G, Purnell MA. 2014. Decay of velvet worms (Onychophora), and bias in the fossil record of lobopodians. BMC Evolutionary Biology. 14, 1–9. doi:10.1186/s12862-014-0222-z.

[32] Schultz TD, Rankin MA. 1985. The ultrastructure of the epicuticular interference reflectors of tiger beetles (*Cicindela*). Journal of Experimental Biology. 117, 87–110.

[33] Mason CW. 1927. Structural colours in insects I. The Journal of physical chemistry. 31, 1856–1872.

[34] Arwin H, Fernández del Río L, Järrendahl K. 2014. Comparison and analysis of Mueller-matrix spectra from exoskeletons of blue, green and red *Cetonia aurata*. Thin Solid Films. 571, 739–743. doi:https://doi.org/10.1016/j.tsf.2014.02.012.

[35] Kurachi M, Takaku Y, Komiya Y, Hariyama T. 2002. The origin of extensive colour polymorphism in *Plateumaris sericea* (Chrysomelidae, Coleoptera). Naturwissenschaften. 89, 295–298. doi:10.1007/s00114-002-0332-0.

[36] Sharma V, Crne M, Park JO, Srinivasarao M. 2009. Structural origin of circularly polarized iridescence in jeweled beetles. Science. 325, 449–451. doi:10.1126/science.1172051.

[37] Parker AR, Mckenzie D, Large M. 1998. Multilayer reflectors in animals using green and gold beetles as contrasting examples. Journal of Experimental Biology. 201, 1307–1313.

For Review Only

[38] Hinton HE, Jarman GM. 1973. Physiological colour change in the elytra of the Hercules beetle, *Dynastes hercules*. Journal of Insect Physiology. 19, 533–549. doi:10.1016/0022-1910(73)90064-4.

[39] Gupta NS, Michels R, Briggs DEG, Evershed RP, Pancost RD. 2006. The organic preservation of fossil arthropods: an experimental study. Proceedings of the Royal Society Series B. 273, 277–2783. doi:10.1098/rspb.2006.3646.

[40] Brink DJ, van der Berg NG, Prinsloo LC, Hodgkinson IJ. 2007. Unusual coloration in scarabaeid beetles. Journal of Physics D: Applied Physics. 40, 2189. doi:10.1088/0022-3727/40/7/050.

[41] Mendoza-Galván A, Fernández del Río L, Järrendahl K, Arwin H. 2018. Graded pitch profile for the helicoidal broadband reflector and left-handed circularly polarizing cuticle of the scarab beetle *Chrysina chrysargyrea*. Scientific Reports. 8, 6456. doi:10.1038/s41598-018-24761-w.

[42] Wagner T, Neinhuis C, Barthlott W. 1996. Wettability and contaminability of insect wings as a function of their surface sculptures. Acta Zoologica. 77, 213–225. doi:10.1111/j.1463-6395.1996.tb01265.x.

[43] Smith DM, Cook A, Nufio CR. 2006. How physical characteristics of beetles affect their fossil preservation. Palaios. 21, 305–310. doi:10.2110/palo.2004.p04-91.

[44] Karr JA, Clapham ME. 2015. Taphonomic biases in the insect fossil record: shifts in articulation over geologic time. Paleobiology. 41, 16–32. doi:10.1017/pab.2014.3.

[45] Smith DM. 2000. Beetle taphonomy in a recent ephemeral lake, Southeastern Arizona. Palaios. 15, 152–160. doi:10.1669/0883-1351(2000)015<0152:BTIARE>2.0.CO;2.

[46] Riek EF; 1970. Chapter 8: Fossil history. In: Insects of Australia: A textbook for students and research workers. Melbourne University Applied Physics Express. p. 168–186.

[47] Poinar GO; 1992. Chapter 6: Implications for biological science. In: Life in amber. Stanford University Press. p. 254–278.

[48] Fernández del Río L, Arwin H, Järrendahl K. 2016. Polarizing properties and structure of the cuticle of scarab beetles from the *Chrysina* genus. Physical Review E. 94, 012409. doi:10.1103/PhysRevE.94.012409.

[49] Vincent JFV. 2002. Arthropod cuticle: a natural composite shell system. Composites Part A: Applied Science and Manufacturing. 33, 1311–1315. doi:10.1016/S1359-835X(02)00167-7.

[50] Stawski D, Rabiej S, Herczynska L, Draczynski Z. 2008. Thermogravimetric analysis of chitins of different origin. Journal of Thermal Analysis and Calorimetry. 93, 489–494. doi:10.1007/s10973-007-8691-6.

For Review Only

[51] Neville AC; 1975. Chapter 3: The structural macromolecules. In: Biology of the Arthropod Cuticle. Springer. p. 71–124.

[52] Blomquist GJ, Dillwith JW; 1985. Chapter 4: Cuticular lipids. In: Kerkut GA, Gilbert LI, editors. Comprehensive insect physiology, biochemistry and pharmacology, Volume 3: Integument, respiration and circulation. Pergamon Press. p. 118–154.

[53] Shamim G, Ranjan S, Pandey D, Ramani R. 2014. Biochemistry and biosynthesis of insect pigments. EJE. 111, 149–164. doi:10.14411/eje.2014.021.

[54] Caveney S. 1971. Cuticle reflectivity and optical activity in scarab beetles: the role of uric acid. Proceedings of the Royal Society of London B: Biological Sciences. 178, 205–225. doi:10.1098/rspb.1971.0062.

[55] Ralph Dennell DS. 1946. A study of an insect cuticle: the larval cuticle of *Sarcophaga falculata* Pand. (Diptera). Proceedings of the Royal Society of London B: Biological Sciences. 133, 348–373. doi:10.1098/rspb.1946.0017.

[56] Briggs DEG. 1999. Molecular taphonomy of animal and plant cuticles: selective preservation and diagenesis. Philosophical Transactions of the Royal Society of London B: Biological Sciences. 354, 7–17. doi:10.1098/rstb.1999.0356.

For Review Only

Tables and table captions

Table 1

		Thickness			Decrease (%)	
Taxon	Layer	untreated (u)	decayed (d)	matured (m)	u/d	u/m
C. boucardi	Epicuticle (µm)	0.2 – 1.0	0.2 – 0.6	0.3– 0.9	33	0
	Outer exocuticle (µm)	11.4 – 14.1	5.3 – 6.4	10.2 – 12.1	54	13
	Inner exocuticle (µm)	3.8 – 6.4	5.0 – 7.0	2.0 – 4.0	18	41
	Lamellae (nm)	100 – 270	70 – 120	170 – 230	49	8
C. gloriosa	Epicuticle (µm)	0.3 – 2.3	0.2 – 2.6	0.4 – 2.0	8	8
	Outer exocuticle (µm)	5.9 – 10.5	4.0 – 7.7	7.2 – 8.7	29	3
	Inner exocuticle (µm)	3.0 – 6.4	12.9 – 16.4	5.2 – 6.3	212	22
	Lamellae (nm)	130 – 240	60 – 160	150 – 190	48	8
I. jamesi	Epicuticle (µm)	0.25 – 1.0	0.5 – 0.7	0.3 – 0.5	4	36
	Outer exocuticle (µm)	13.0 – 16.4	8.2 – 10.5	9.4 – 11.3	36	30
	Inner exocuticle (µm)	7.2 – 10.0	18.7 – 20.3	7.0 – 8.7	127	9
	Lamellae (nm)	110 – 200	130 – 190	120 – 170	3	6
G. virens	Epicuticle(µm)	0.2 – 0.7	0.2 – 0.5	0.1 – 0.3	22	56
	Exocuticle (µm)	5.4 – 13.7	5.4 – 8.8	8.6– 13.9	26	18
	Lamellae (nm)	90 – 200	90 – 160	100– 230	14	14
T. flammea	Epicuticle(µm)	0.4 – 0.6	0.6 – 0.9	0.3 – 0.4	50	30
	Exocuticle (µm)	18.6 – 24.4	27.5 – 27.8	17.8 –20.5	29	11
	Lamellae (nm)	130 – 210	140 – 200	130–240	0	9

Table 2

Taxon *[region]*	Lamellar thickness (nm)	$\lambda_{theoretical}$ (nm)	$\lambda_{experimental}$(nm)	Difference (%)
C. boucardi [green]	175 (+232)	546	584	+ 6.7
C. gloriosa [green]	172	537	530	- 1.3
I. jamesi [green]	185	577	550	- 4.9
I. jamesi [red]	203	633	636	+ 0.3
G. virens [green]	152	474	507	+ 6.5
T. flammea [green]	173	540	533	- 1.5

Table 1: Thicknesses of cuticular components measured manually from scanning electron micrographs of green cuticle. Data are based on at least ten measurements from two different images.

Table 2: Experimental and theoretical maximum reflection wavelengths of green and red regions of untreated elytra. Lamellar thicknesses are from FFT of scanning electron micrographs; theoretical maximum reflection wavelengths are from Bragg's equation, using a refractive index for chitin of 1.56 and the lamellar thicknesses from FFT.

For Review Only

Figure captions

Figure 1: Photographs of the five scarab taxa studied, with and without polarizing filters, on untreated, decayed and matured cuticle. Scale in the left-hand column: 20 mm (except *G. virens*: 10 mm); scale in the right-hand column: 5 mm.

Figure 2: Light- and scanning electron micrographs of the surface of untreated, decayed and matured elytra. Scale: 50 µm for light micrographs (LM) and 10 µm for scanning electron micrographs (SEM).

Figure 3: Reflectance spectra from untreated (solid black), decayed (red dash) and matured (blue dot) samples of beetle elytra. The spectra were chosen as mostly representative as possible of the global results.

Figure 4: Mueller matrix 41 obtained on degraded cuticle: (a) from untreated (solid black), decayed (red dash) and matured (blue dot) samples of *C. boucardi,* (b) from untreated (solid black), decayed (red dash) and matured (blue dot) samples of *I. jamesi*, (c) from temperature-series maturation of *C. boucardi* and (d) from temperature-series maturation of *I. jamesi*.

Figure 5: SEM micrographs of longitudinal cross-sections through untreated, decayed and matured elytra, showing the epicuticle and part of the outer exocuticle. Scale: 2 µm.

Supplementary information, Figure 1: Light micrographs of decayed elytra of *C. gloriosa* and *C. boucardi*. Scale: 5 mm.

Supplementary information, Figure 2: Light micrographs of elytra of *C. boucardi*, *C. gloriosa*, *I. jamesi* and *T. flammea* matured (a) wrapped in polytetrafluoroethylene, (b) unwrapped. Scale: 2 mm.

Supplementary information, Figure 3: Light micrographs of *C. boucardi* and *T. flammea* elytra treated with(a) KOH, (b) H_2SO_4 and (c) H_2O_2. Images of *T. flammea* treated with H_2O_2 were taken immediately (left- green iridescence) and one week (right- blue iridescence) after the experiment. Scale: 1 mm.

For Review Only

Supplementary information, Figure 4: Spectrophotometric data from untreated (black), decayed (red) and matured (blue) cuticle. Box and whiskers plots show the range of local λ_{max} values obtained from reflectance spectra: square: mean, crosses: minimum and maximum values, n: number of measurements, SD: standard deviation.

Supplementary information, Figure 5: Mueller matrix elements recorded at 20 ° on *C. boucardi* (a,c) and *I. jamesi* (b,d). (a, b): untreated (solid black), decayed (red dash) and matured (blue dot) samples (c,d): temperature-series maturation.

Supplementary information, Figure 6: Schematic drawings and SEM micrographs of longitudinal cross-sections of untreated, decayed and matured elytra, showing the epicuticle, the outer exocuticle and part of the inner exocuticle. Scale: 5 µm.

For Review Only

Ischipsopha jamesi jamesi

Under Review for J.R. Soc. Interface

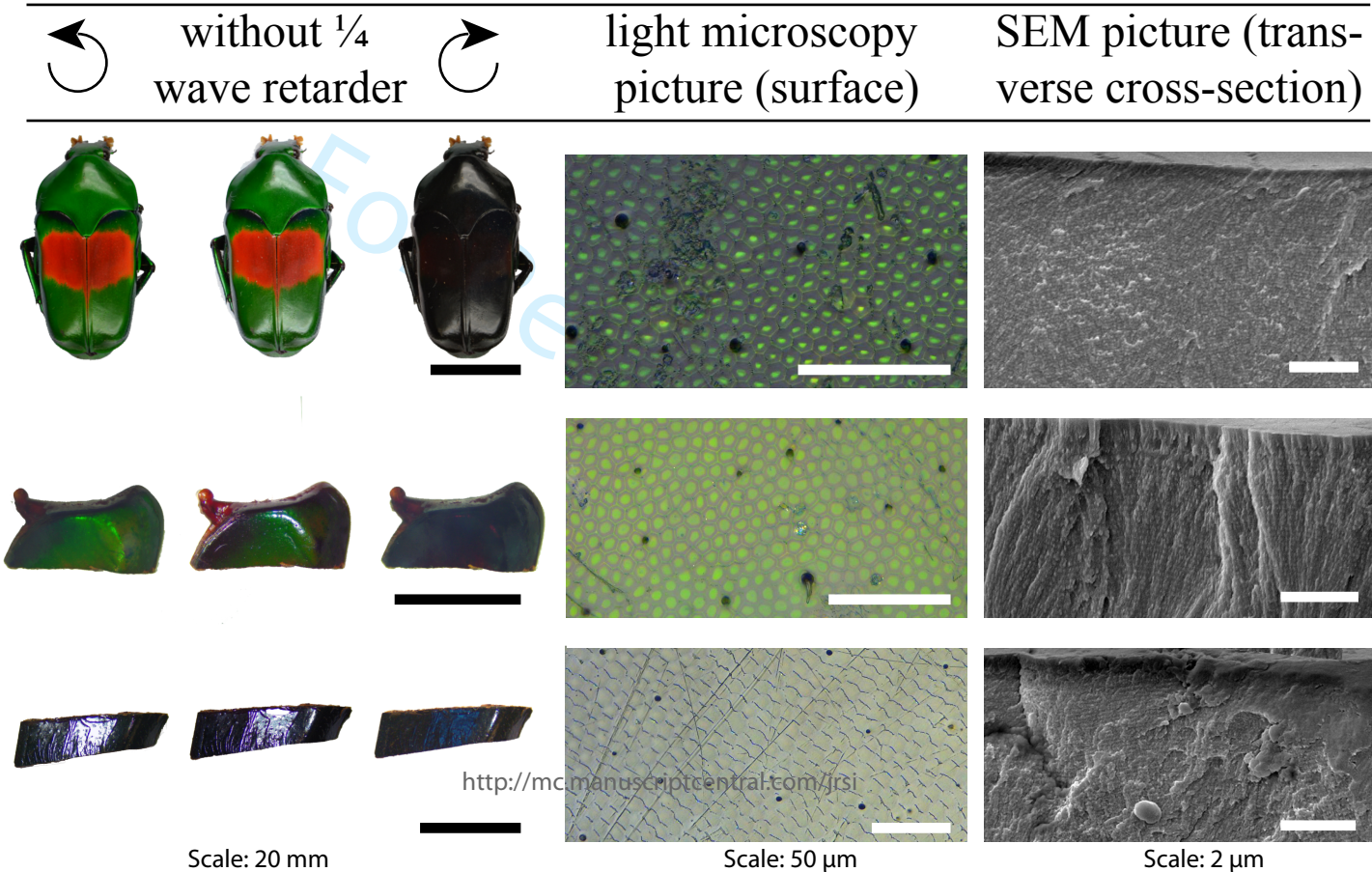

http://mc.manuscriptcentral.com/jrsi